



IL-1 β derived from mixed-polarized macrophages activates fibroblasts and synergistically forms a cancer-promoting microenvironment

Jun Zhang^{1,2} · Lingfeng Fu^{1,2} · Noriko Yasuda-Yoshihara^{1,2} · Atsuko Yonemura^{1,2} · Feng Wei^{1,2} · Luke Bu^{1,2} · Xichen Hu^{1,2} · Takahiko Akiyama^{1,2} · Fumimasa Kitamura^{1,2} · Tadahito Yasuda^{1,2} · Takashi Semba^{1,2} · Tomoyuki Uchihara^{1,2} · Rumi Itoyama^{1,2} · Kohei Yamashita¹ · Kojiro Eto¹ · Shiro Iwagami¹ · Masakazu Yashiro³ · Yoshihiro Komohara⁴ · Hideo Baba^{1,5} · Takatsugu Ishimoto^{1,2}

Received: 18 July 2022 / Accepted: 15 November 2022 / Published online: 13 December 2022

© The Author(s) under exclusive licence to The International Gastric Cancer Association and The Japanese Gastric Cancer Association 2022

Abstract

Background Remodeling the tumor microenvironment (TME) to benefit cancer cells is crucial for tumor progression. Although diffuse-type gastric cancer (DGC) preferentially interacts with the TME, the precise mechanism of the complicated network remains unknown. This study aimed to investigate the mutual activation mechanism underlying DGC progression.

Methods Mass cytometry analysis of co-cultured macrophages, noncancerous fibroblasts (NFs), and DGC cells was performed. RNA sequencing was applied to examine gene expression in fibroblasts. DGC cells were treated with cytokines to examine their effect on characteristic changes. The TCGA and Kumamoto University cohorts were used to evaluate the clinical relevance of the in vitro findings.

Results Cohort analysis revealed that DGC patients had a poor prognosis. The fibroblasts and macrophages interacted with DGC cells to form a cell cluster in the invasive front of DGC tissue. The original 3D triple co-culture system determined the promotional effects of nonmalignant cells on DGC invasive growth. We notably identified a mixed-polarized macrophage cell type with M1/M2 cell surface markers in a triple co-culture system. IL-1 β from mixed-polarized macrophages induced the conversion of NFs to cancer-associated fibroblast-like (CAF-like) cells, promoting the malignant phenotype of DGC cells by inducing the secretion of IL-6, IL-24, and leukemia inhibitory factor (LIF). Moreover, IL-6 and colony stimulating factor 2 (GM-CSF) cooperated to maintain the stable state of mixed-polarized macrophages. Finally, we found that mixed-polarized macrophages were frequently detected in DGC tissues.

Conclusion These findings demonstrated that mixed-polarized macrophages exist as a novel subtype through the reciprocal interaction between DGC cells and nonmalignant cells.

✉ Hideo Baba
hdobaba@kumamoto-u.ac.jp

✉ Takatsugu Ishimoto
taka1516@kumamoto-u.ac.jp

¹ Department of Gastroenterological Surgery, Graduate School of Medical Sciences, Kumamoto University, 1-1-1 Honjo, Chuo-Ku, Kumamoto 860-8556, Japan

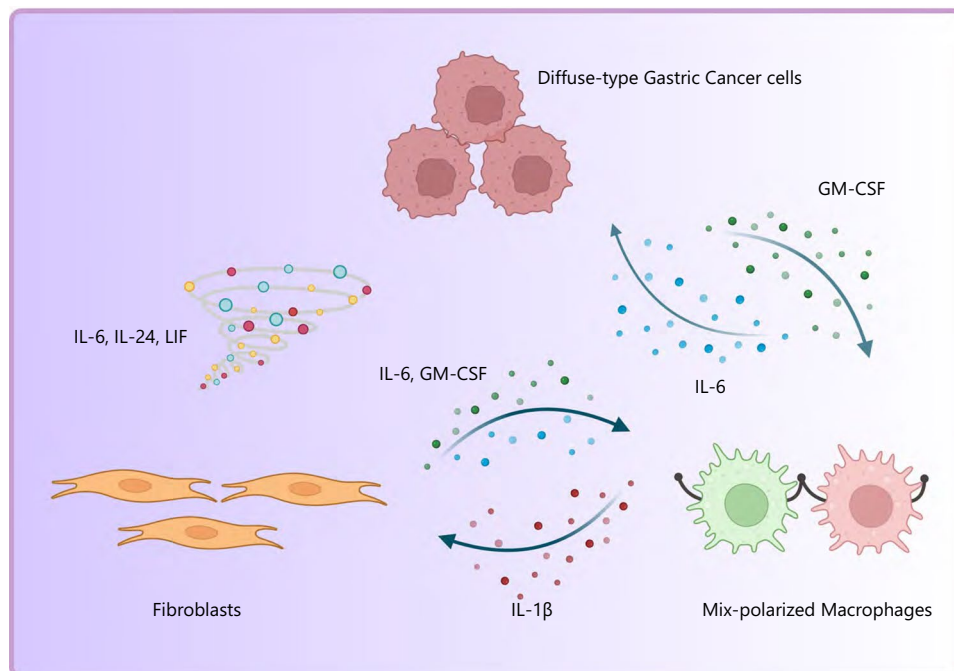
² Gastrointestinal Cancer Biology, International Research Center of Medical Sciences (IRCMS), Kumamoto University, Kumamoto, Japan

³ Department of Molecular Oncology and Therapeutics, Osaka Metropolitan University Graduate School of Medicine, Osaka, Japan

⁴ Department of Cell Pathology, Kumamoto University, Kumamoto, Japan

⁵ Center for Metabolic Regulation of Healthy Aging, Faculty of Life Sciences, Kumamoto University, Kumamoto, Japan

Graphical Abstract



Keywords Tumor microenvironment · Diffuse-type gastric cancer · Fibroblast · Mixed-polarized macrophage · Mass cytometry

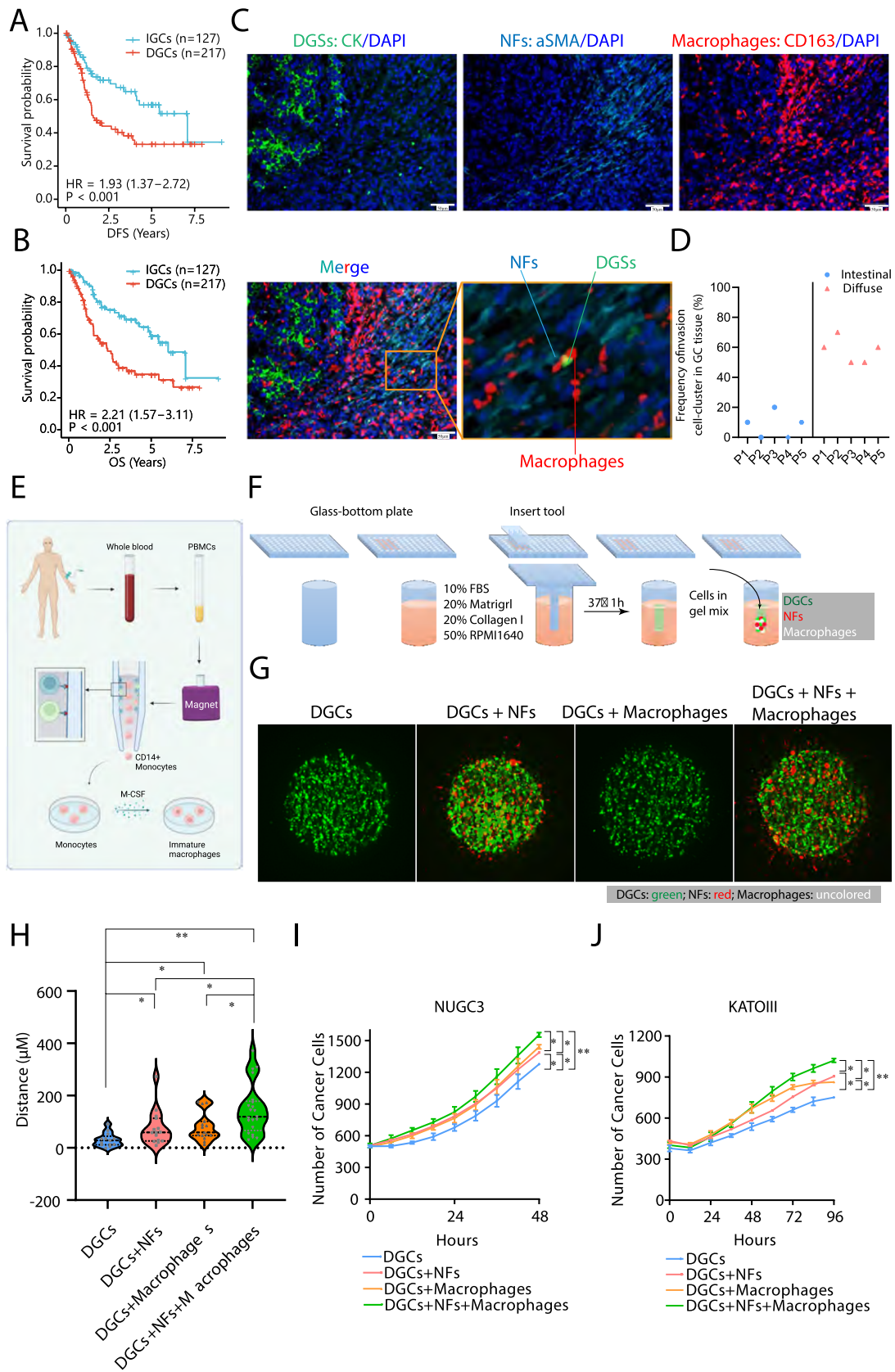
Abbreviations

| | |
|--------|---|
| GC | Gastric cancer |
| DGC | Diffuse-type gastric cancer |
| IGC | Intestinal-type gastric cancer |
| TME | Tumor microenvironment |
| NFs | Noncancerous fibroblasts |
| TCGA | The Cancer Genome Atlas |
| CAF | Cancer-associated fibroblast |
| TAMs | Tumor-associated macrophages |
| ECM | Extracellular matrix |
| LIF | Leukemia inhibitory factor |
| GM-CSF | Colony stimulating factor 2 |
| DFS | Disease-free survival |
| OS | Overall survival |
| GS | Genomically stable |
| PBMCs | Peripheral blood mononuclear cells |
| MACS | Magnetic-activated cell sorting |
| t-SNE | T-distributed stochastic neighbor embedding |
| DEGs | Differentially expressed genes |
| GO | Gene Ontology |
| KEGG | Kyoto Encyclopedia of Genes and Genomes |

Background

Gastric cancer (GC) is a common malignant tumor in the digestive system with high morbidity and mortality, especially in Asia [1]. Although the development of molecular targeted therapies and novel immunotherapies has begun to

Fig. 1 Nonmalignant cells enhanced the invasive growth of DGC cells through direct interaction. **A.** DFS curves of all patients with gastric cancer based on Lauren's classification. **B.** OS curves of all patients with gastric cancer based on Lauren's classification. **C.** Representative immunofluorescence staining of NFs and macrophages clustered around invasive-front GC cells. The NFs, macrophages and DGCs were stained with aSMA, CD163 and cytokeratin, respectively; nuclei were stained with DAPI. The merged image of aSMA, CD163 and cytokeratin staining and DAPI nuclear staining is shown in the bottom panel. Scale bars: 50 μ m. **D.** The invasive-front cell cluster was more enriched in DGCs than in IGCs. **E.** Workflow via which CD14⁺ monocytes are sorted from whole blood. Monocytes were treated with M-CSF (50 ng/ml) to induce their differentiation into macrophages. **F.** Protocol for designing the original 3D triple co-culture model. **G.** Cells were seeded into the Matrigel holes in different combinations, and the movement distances of DGC cells in the hole were recorded (DGCs: green; NFs: red; macrophages: uncolored). **H.** Statistical analysis of the movement distances of cells in the different groups. NFs and macrophages promoted DGC cell migration, and the triple co-culture had the most significant gain effect. **I, J.** Growth assay of 2 DGC lines co-culture with NFs and macrophages in different combinations. *, $P < 0.05$; **, $P < 0.01$; ***, $P < 0.001$



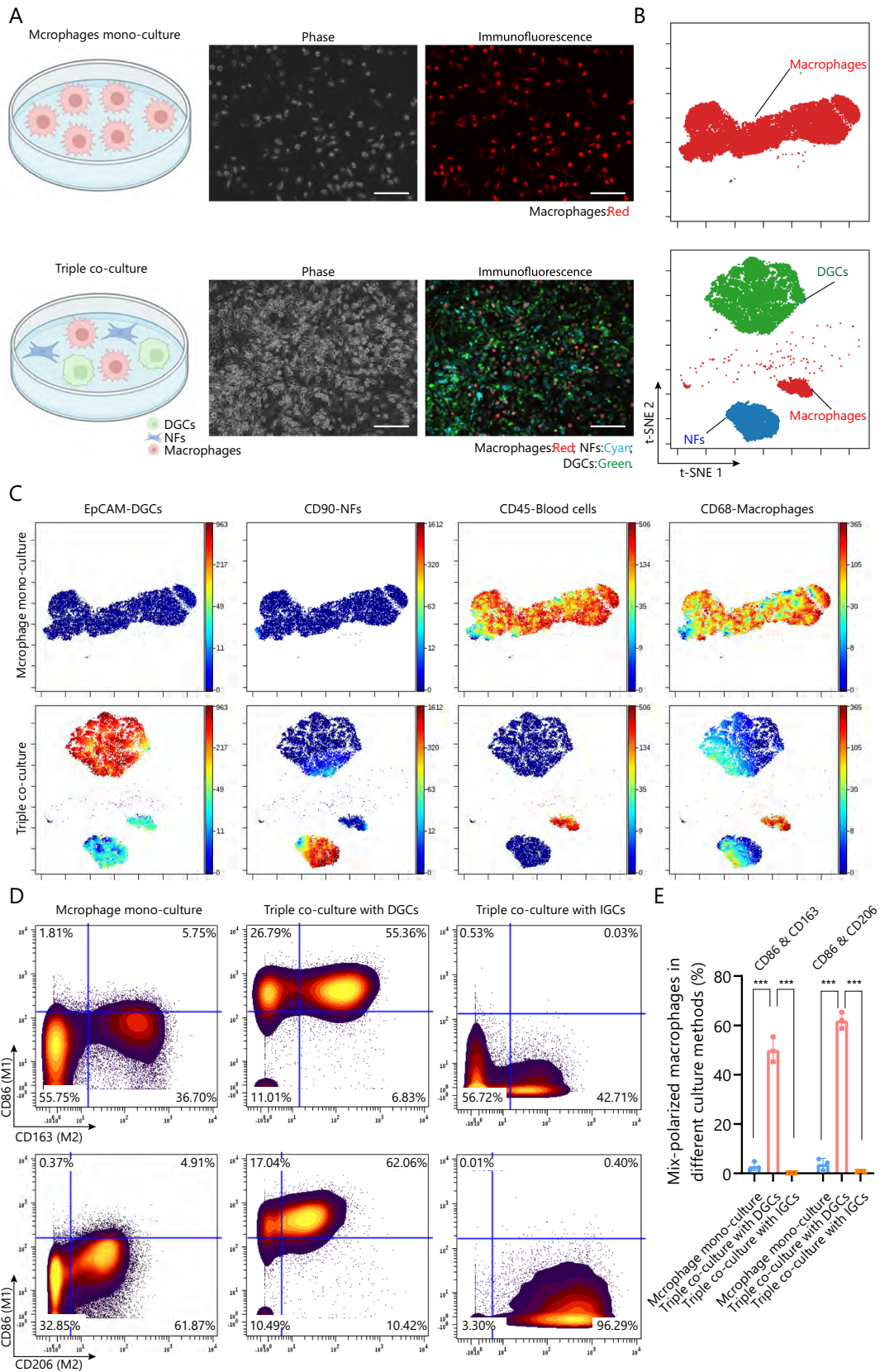


Fig. 2 Mix-polarized macrophages existed stably in the triple co-culture system. **A.** Schematic illustrating the cell mono-culture and triple co-culture procedures (left). Representative images of phase contrast (middle) and immunofluorescence (right) staining of macrophages in different culture conditions. Scale bars: 200 μ m. **B.** The single cells were projected onto the *t*-SNE plot. The *t*-SNE algorithm distinguished the different cell clusters in the triple co-culture system. **C.** Heatmap of the *t*-SNE plots with labeled populations (CD90, EpCAM, CD45, and CD 68) distinguishing various cell clusters. The colors show the row-normalized Z scores of gene expression values. **D.** Compared to mono-cultured macrophages, more macrophages simultaneously expressed M1 (CD86) and M2 (CD163, CD206) markers in the triple co-culture system. These cells were classified as mixed-polarized macrophages. **E.** The proportion of mixed-polarized macrophages among mono-cultured, triple co-cultured with DGCs (55.36 and 62.06%) and with IGCs (0.03 and 0.40%)

update the cancer treatment paradigm, the response rate of GC patients remains limited [2, 3]. Therefore, the prognosis of patients with advanced GC who are treated with comprehensive therapy does not reach expectations [4]. Intratumoral heterogeneity and plasticity may contribute to GC progression and therapeutic resistance [5]. According to Lauren's classification, GCs are divided into two subtypes, intestinal-type GCs (IGCs) and diffuse-type GCs (DGCs), based on their histological structures [6]. As poorly cohesive cancer cells tend to grow invasively, DGCs are likely to lead to unresectable metastasis and peritoneal dissemination, leading to a worse prognosis. In addition, The Cancer Genome Atlas (TCGA) classification of GC shows extensive overlap between DGCs and genomically stable (GS) groups [7]. This finding indicates that the aggressive phenotype of DGCs may be affected by the tumor microenvironment (TME).

The TME in advanced cancers contains stromal cells and immune cells that enhance cancer progression and resistance to treatment [8]. One major aspect of cancer biology is the interactions between tumor cells and nonmalignant cells in the TME. Bidirectional communication alters cell subset distributions [9]. Cancer-associated fibroblasts (CAFs), a major population in the TME, are more genetically stable than cancer cells, as determined by the exome sequencing of isolated CAF libraries followed by mutation analysis; thus, the characteristics of fibroblasts are determined by transcriptional alterations [10].

On the other hand, macrophages infiltrating the TME (tumor-associated macrophages; TAMs) expedite tumor growth, angiogenesis, immune evasion, and remodeling of the extracellular matrix (ECM) to facilitate GC metastasis [11]. Macrophages derived from monocytes were categorized into proinflammatory M1 and tissue-repairing M2 phenotypes with anti- and protumorigenic functions, respectively [12, 13]. Furthermore, fibroblast-macrophage interactions centered on the colony stimulating factor (CSF)-colony stimulating factor receptor (CSFR) axis are widespread in

healthy tissue and in inflammatory conditions such as fibrosis and cancer. Noncancerous fibroblasts (NFs) support macrophages in a niche via the provision of CSFs, which promote the survival or signal expression of a macrophage-specific transcriptional program. Under inflammatory conditions, NFs continue to provide CSFs as an essential factor for macrophages [14].

Although fibroblasts and macrophages are critical components of the TME that drive cancer, the interaction among three kinds of cells, including cancer cells, is extremely complicated. This study aimed to investigate the orchestrated effect of DGCs, macrophages, and fibroblasts in the TME. We created an original 3D triple co-culture system to mimic the TME and determined the cellular state of macrophages and fibroblasts through reciprocal interaction with DGC cells.

Materials and methods

Cell lines and culture

Human DGC cell lines were purchased from the RIKEN BioResource Center Cell Bank (KATO III) and the Japanese Collection of Research Bioresources Cell Bank (NUGC3). OCUM-2MD3 was derived from a peritoneal-metastatic nodule after orthotopic implantation of OCUM-2 M [15]. NFs were obtained from the non-tumor gastric wall tissues of GC patients [16, 17]. Peripheral blood mononuclear cells (PBMCs) were obtained from the whole blood of healthy volunteers by centrifugation. Magnetic-activated cell sorting (MACS) was used to acquire CD14+ monocytes from PBMCs and induce them to differentiate into immature macrophages by M-CSF (colony stimulating factor 1, 50 ng/ml, Fig. 1E).

Statistical analysis

All experiments were performed in triplicate, and the data are presented as the mean \pm standard deviation. Data were analyzed using GraphPad Prism 9.0. *P* values < 0.05 were considered statistically significant.

Results

Nonmalignant cells enhance the invasive growth of DGC cells through direct interaction

IGC tissues exhibit distinct glandular duct structures, and the basement membrane blocks the direct interaction of fibroblasts and macrophages with GC cells. In contrast, DGCs with locally disintegrated structures lose this barrier,

facilitating direct communication between GC cells and non-malignant cells in the TME. Survival analysis confirmed that patients with DGCs had worse disease-free survival (DFS, Fig. 1A) and overall survival (OS, Fig. 1B) rates than those with IGCs in surgically resected tissues from 344 patients of the Kumamoto University cohort. Given this result, we expected that the interaction between the TME and tumor cells would be an important factor accounting for the poor prognosis of DGC patients. Subsequently, we randomly selected 5 DGC and 5 IGC patients for multiple staining to compare the differences in TME between the two subtypes. In DGCs, fibroblasts and macrophages tended to aggregate with DGC cells and formed cell clusters at the invasion front (Fig. 1C and D). In contrast, cancer cells maintain the glandular structures in IGCs and there were almost no invasive cell clusters formed by the three cells (Sup Fig. 1 and Fig. 1D). Given the finding in human DGC tissue, we conducted an in vitro assay using DGC cells, macrophages and fibroblasts to show the significance of nonmalignant cells in the cancerous behavior of DGC cells.

We first obtained PBMCs from the whole blood of healthy volunteers by centrifugation. MACS was used to obtain CD14⁺ monocytes from the PBMCs, and these monocytes were treated with M-CSF to induce their differentiation into immature macrophages (Fig. 1E). NFs were acquired by the primary culture of cells from noncancerous tissues surrounding cancerous tissues in GC surgical specimens [16, 17]. Then, we designed a 3D triple co-culture model to analyze the influence of NFs and macrophages on DGC invasion (Fig. 1F). The cells were seeded into the Matrigel holes in different combinations and are shown as different colors (DGCs: green; NFs: red; macrophages: uncolored). Mono-cultured DGCs were used as a control. The movement distance of DGC cells in the Matrigel hole was recorded. Regardless of which type of co-culture promoted DGC migration, as expected, the triple co-culture had the most significant gain effect (Fig. 1G, H Sup Fig. 2A, B supplementary movie 2).

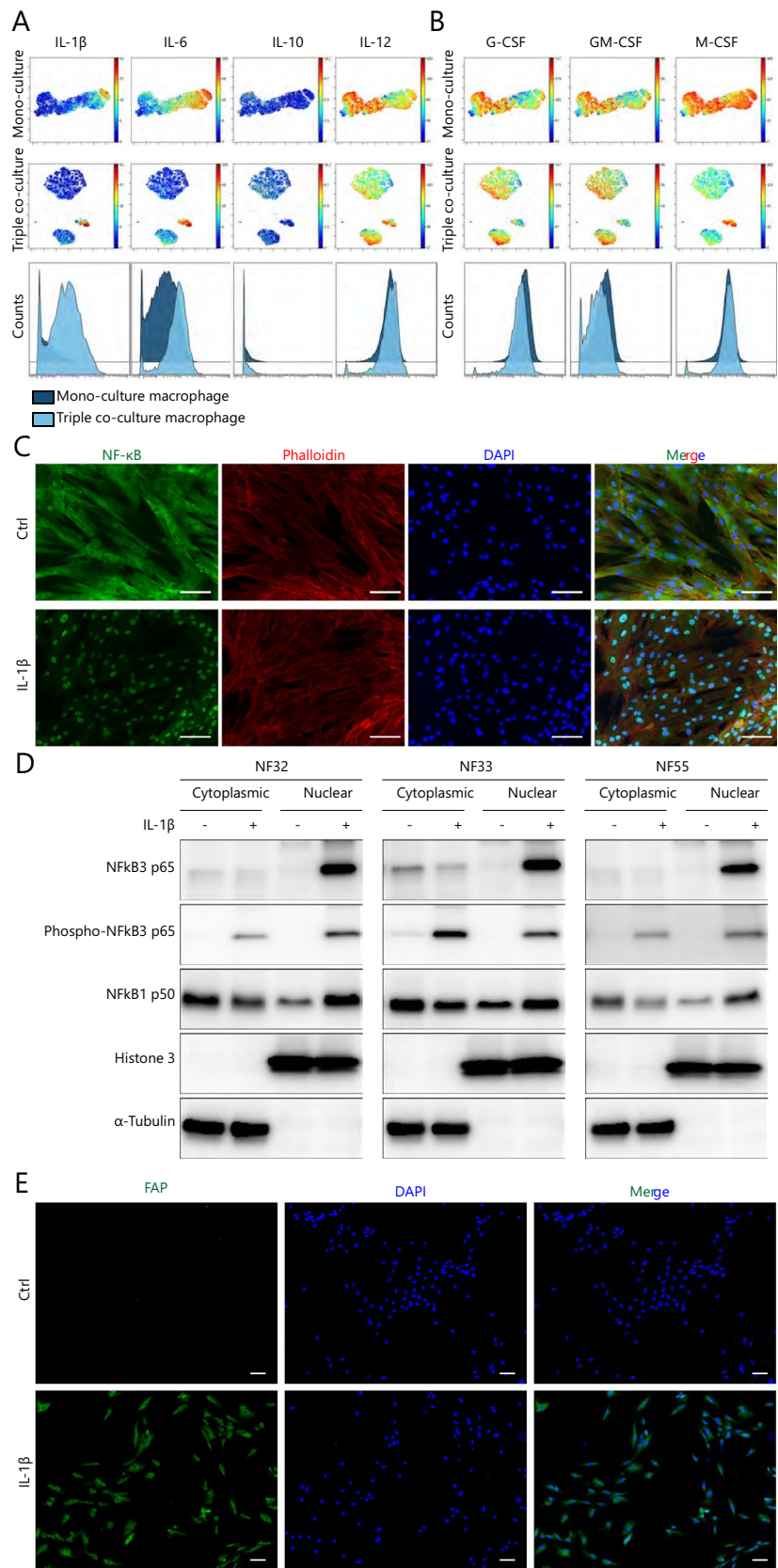
In addition, we also evaluated the effect of co-culture on DGC proliferation. Similar to migration, nonmalignant cells enhanced DGC cell growth. In particular, growth was remarkably promoted by triple co-culture (Fig. 1I and J). These findings suggested that multicellular interactions among the three kinds of cells affected the characteristics of the DGC cells. Therefore, it was imperative to further evaluate the molecular mechanism of DGC cell invasive growth under triple co-culture conditions.

Mixed-polarized macrophages exist stably in the triple co-culture system

Cancer cells communicate with nonmalignant cells through cytokines and jointly reshape the

microenvironment to adapt to their growth. Therefore, the identification of the cytokine source in a co-culture system is the bottleneck in elucidating the mechanism of cell interaction. Given our previous knowledge that NFs are activated by proinflammatory cytokines [10], we first focused on the mechanism of macrophage activation in the triple co-culture system (Fig. 2A). To do this, the membrane and secreted proteins of macrophages cultured alone (mono-culture) and macrophages in the triple co-culture system were examined by mass cytometry. Eight membrane proteins were used to identify the cell source: EpCAM for GC cells; CD90 and PDGFR α for fibroblasts; and CD14, CD45, CD206, CD163, and CD86 for macrophages. In particular, CD86 and IL-12 (M1 macrophage markers) and CD206, CD163 and IL-10 (M2 macrophage markers) were utilized to distinguish the subgroups of macrophages. Moreover, 11 secreted proteins and cell surface markers were examined. Single cells were projected to the *t*-SNE distribution to reduce the dimensions and distinguish the cell clusters [18]. Each cell subtype in the triple co-culture system was identified by the *t*-SNE algorithm (Fig. 2B). We first confirmed that each population was distinguished by the expression of the following representative lineage markers: EpCAM for DGC cells, CD90 for NFs, and CD45/CD68 for macrophages (Fig. 2C). To further investigate the polarization of macrophages in the triple co-culture, M1 macrophage markers (CD86) and M2 macrophage markers (CD163 and CD206) were analyzed. Notably, we found that mixed-polarized macrophages expressing both M1/M2 cell surface markers (CD86/CD163 or CD86/CD206) were dominant in the triple co-culture system when macrophages were co-culture with DGC cells and NFs (Fig. 2D, middle). However, when macrophages were co-cultured with IGC cells and NFs, there was no mixed polarization type (Fig. 2D, right). This finding suggested that the proportion of mixed-polarized macrophages was markedly increased via their interaction with the other two cell types, especially with DGCs (Fig. 2E). In general, macrophages are classically divided into two subtypes, M1 and M2, based on studies using murine macrophages. Since macrophage polarization seems to be more complicated in humans, the descriptions of “M1-like” or “M2-like” were used to refer to the macrophage phenotypes. Nevertheless, this classification was arbitrary and ignored the plasticity of macrophages. Given the finding in the triple co-culture system, we speculated that mixed-polarized macrophages were more widespread in the TME than the extreme M1 and M2 macrophages.

Fig. 3 Mix-polarized macrophages contributed to NF activation. **A.** The *t*-SNE plot and histograms showing the expression of IL-1 β , IL-6, IL-10 and IL-12 in mono-culture and triple co-culture cells. IL-1 β was overexpressed in triple-cultured macrophages. **B.** The expression of G-CSF, GM-CSF, and M-CSF in mono-culture and triple co-culture systems. **C.** Immunofluorescence staining of NF- κ B, phalloidin and DAPI in NFs before and after treatment with IL-1 β for 30 min. IL-1 β induced the translocation of NF- κ B from the cytoplasm to the nucleus and activated the NF- κ B pathway. Scale bars, 50 μ m. **D.** Western blot analysis of p65, p50, and phospho-p65 in the NF cytoplasm and nucleus. NFs were untreated or treated with IL-1 β for 30 min. **E.** Immunofluorescence staining of FAP and DAPI in NFs before and after treatment with IL-1 β . IL-1 β increased FAP expression



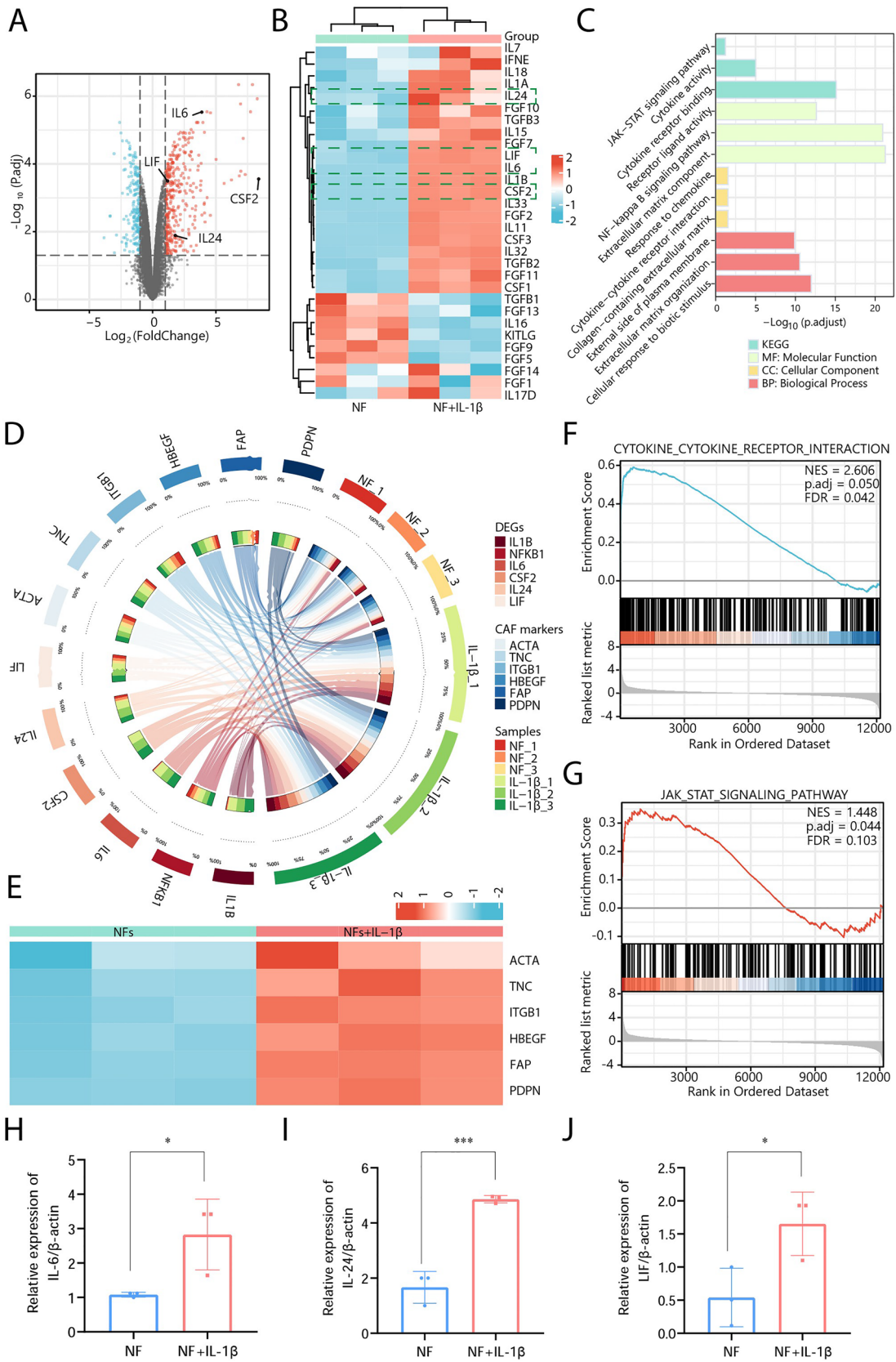


Fig. 4 IL-1 β enhanced the expression of NF-derived cytokines. **A.** Volcano plot showing the DEGs in 3 NF cell lines 1 day after IL-1 β treatment. A total of 590 genes were identified, among which 382 were upregulated and 208 were downregulated in IL-1 β -treated NFs (red: upregulated; blue: downregulated). **B.** Heatmap showing higher IL-6, IL-24, LIF, and CSF2 levels in IL-1 β -treated NFs than in untreated NFs. **C.** Gene ontology and pathway analyses revealed that cytokine–cytokine receptor interactions were promoted by IL-1 β . **D.** Circos plot of the syntenic relationships among candidate biomarkers, CAF-related genes, and the samples. **E.** Heatmap showing that CAF-associated markers were overexpressed in IL-1 β -treated NFs. **F, G.** GSEA graphs of the upregulated cytokine–cytokine receptor interaction and JAK-STAT signaling pathway signatures in 3 NF lines 1 day after IL-1 β treatment. **H, I, J.** The mRNA expression of IL-6, IL-24, and LIF in NFs and IL-1 β -treated NFs. *, $P < 0.05$; **, $P < 0.01$; ***, $P < 0.001$

Mix-polarized macrophages contribute to the activation of NFs

To next assess the function of mixed-polarized macrophages in the TME, we analyzed the expression of macrophage-derived cytokines by mass cytometry to verify the mechanism by which mixed-polarized macrophages activate NFs and DGCs in the triple co-culture system. We intensively examined the expression of interleukin- and CSF-related molecules associated with macrophages. Among these cytokines, IL-1 β levels were higher in co-cultured macrophages than in mono-cultured macrophages (Fig. 3A and B), suggesting that IL-1 β production was a feature of mixed-polarized macrophages.

To examine the effect of IL-1 β derived from mixed-polarized macrophages on NFs, we treated NFs with IL-1 β and examined NF- κ B signaling as a downstream target of IL-1 β . Importantly, the activation of NF- κ B signaling is an essential indicator of CAFs [19]. Therefore, we first assessed the localization of p65 by immunofluorescence analysis and observed the nuclear translocation in NFs treated with IL-1 β (Fig. 3C). Similarly, Western blotting analysis confirmed that IL-1 β promoted the translocation of p65 and p50 into the nucleus and induced the phosphorylation of p65 in three independent NFs (Fig. 3D). Subsequently, we stained fibroblast activation protein alpha (FAP), a marker of CAFs, in NFs with or without IL-1 β . FAP was barely expressed in NFs, while the expression was significantly increased by IL-1 β treatment (Fig. 3E). These results suggested that IL-1 β successfully activated NF- κ B signaling in NFs, indicating CAF-like cells.

IL-1 β enhances the expression of NF-derived cytokines

Subsequently, RNA-seq was applied to identify the transcriptome changes in IL-1 β -treated NFs. We analyzed DEGs in IL-1 β -treated NF samples compared with NF samples.

We identified a total of 590 DEGs, of which 382 genes were upregulated and 208 genes were downregulated in IL-1 β -treated NFs (Fig. 4A). The accompanying heatmap revealed the DEGs related to cytokines and growth factors (Fig. 4B). IL-6, CSF2, IL-24, and LIF were upregulated in IL-1 β -treated NFs, and pathway analysis revealed that the cytokine–cytokine receptor interaction was promoted by IL-1 β treatment (Fig. 4C). Next, we evaluated the similarities of IL-1 β -treated NFs and CAFs at the molecular level. We included the target molecules in the analysis and selected common CAF-related markers as controls (ACTA, TNC, ITGB1, HBEGF, FAP, and PDPN) [20]. The expression of CAF-related molecular markers was significantly elevated by IL-1 β treatment (Fig. 4D and E). Furthermore, the areas shown on the right side of Fig. 4D represent the expression levels of these genes in each sample. The area of the IL-1 β -treated samples was larger than that of the NF samples, and the area of the chord represents the correlation between gene expression and the samples. These results suggested that the secreted phenotype reflected the conversion of CAFs from NFs under IL-1 β stimulation.

To strengthen the pathway analysis results, we conducted GSEA of the DEGs and demonstrated that genes related to the "CYTOKINE CYTOKINE RECEPTOR INTERACTION" and "JAK-STAT SIGNALING PATHWAY" were enriched in IL-1 β -treated NFs (Fig. 4F and G). We also confirmed that IL-1 β significantly increased the expression of IL-6, IL-24 and LIF in NFs by qRT-PCR (Fig. 4H–J). Taken together, these data show that IL-1 β induced the transformation of NFs and promoted the expression of IL-6, IL-24, and LIF, indicating reshaping of the TME.

Activated NF-derived factors promote DGC invasive growth

Cell growth and migration assays were performed to assess the effects of different cytokines on the malignant phenotype of DGCs. The proliferation curves of both DGC cell line (NUGC3 and KATO III) showed that all three cytokines (IL-6, IL-24, and LIF) induced cell growth (Fig. 5A and B). Next, we assessed changes in the motility of DGC cells treated with IL-6, IL-24, and LIF. Real-time imaging recorded the motion statuses of the cells over 48 h (Supplementary movies 3 and 4). The migration trial and migration average traveled distances revealed that all three cytokines promoted the motility of NUGC3 cells and that IL-6 and IL-24, but not LIF, accelerated the motility of KATO III cells (Fig. 5C and D).

IL-6, IL-24, and LIF are known to activate the JAK/STAT pathway in several types of cells [21–23]. Therefore, we examined whether these factors could activate

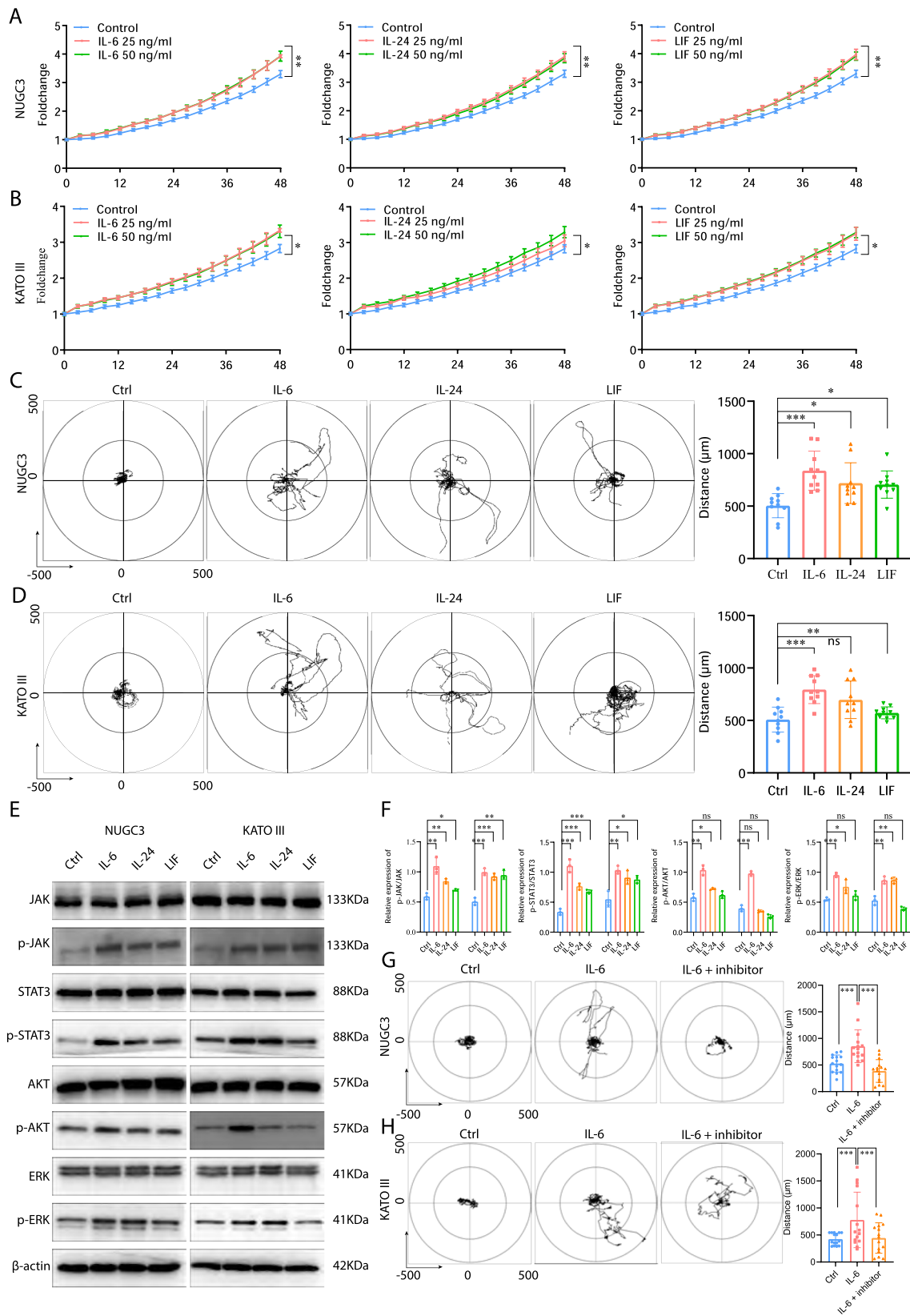


Fig. 5 Activated NF-derived factors promoted DGC invasive growth. **A, B.** Growth assay of 2 DGC cell lines treated with or without IL-6, IL-24, and LIF (50 ng/ml). The cytokines promoted DGC cell proliferation. **A.** NUGC-3; **B.** KATO III. **C, D.** Migration patterns and migration average traveled distances of DGC cells treated with or without IL-6, IL-24, and LIF for 48 h. Left, migration patterns; Right, average distances. **E, F.** Western blot analysis of the p-JAK, p-STAT3, p-ERK, and p-AKT levels in NUGC3 and KATO III3 cells. Cells were untreated or treated with IL-6, IL-24, and LIF for 30 min. **G, H.** Migration patterns and migration average traveled distances of DGC cells treated with IL-6 and JAK/STAT inhibitor for 48 h. Left, migration patterns; Right, average distances. ns, not significant; *, $P < 0.05$; **, $P < 0.01$; ***, $P < 0.001$.

the phosphorylation pathway in NUGC3 and KATO III cells. Consequently, all three cytokines successfully induced the phosphorylation of JAK and STAT3 in both DGC cell lines. Moreover, IL-6 and IL-24 activated AKT phosphorylation in the PI3K/AKT pathway and ERK phosphorylation in the MAPK pathway (Fig. 5E and F). Subsequently, a JAK/STAT inhibitor, WP1066, was used to assess the role of the IL-6/JAK/STAT axis in the migration ability of DGC cells. As expected, the migration of cells was significantly decreased by adding WP1066, suggesting that WP1066 effectively antagonized the tumor-promoting effect of IL-6 (Fig. 5G and H).

NFs and DGC maintain the stability of mixed-polarized macrophages

In the DGC cell triple co-culture system, we discovered the existence of NFs and DGC cells were obviously involved in the mixed polarization of macrophages. Moreover, mixed-polarized macrophages further adjusted the TME and exacerbated the malignant phenotype of DGC cells. Therefore, to some extent, the mix-polarized macrophages were closer to the definition of TAMs, and the molecular mechanism by which the TME synergistically induced mix-polarized polarization needs to be clarified.

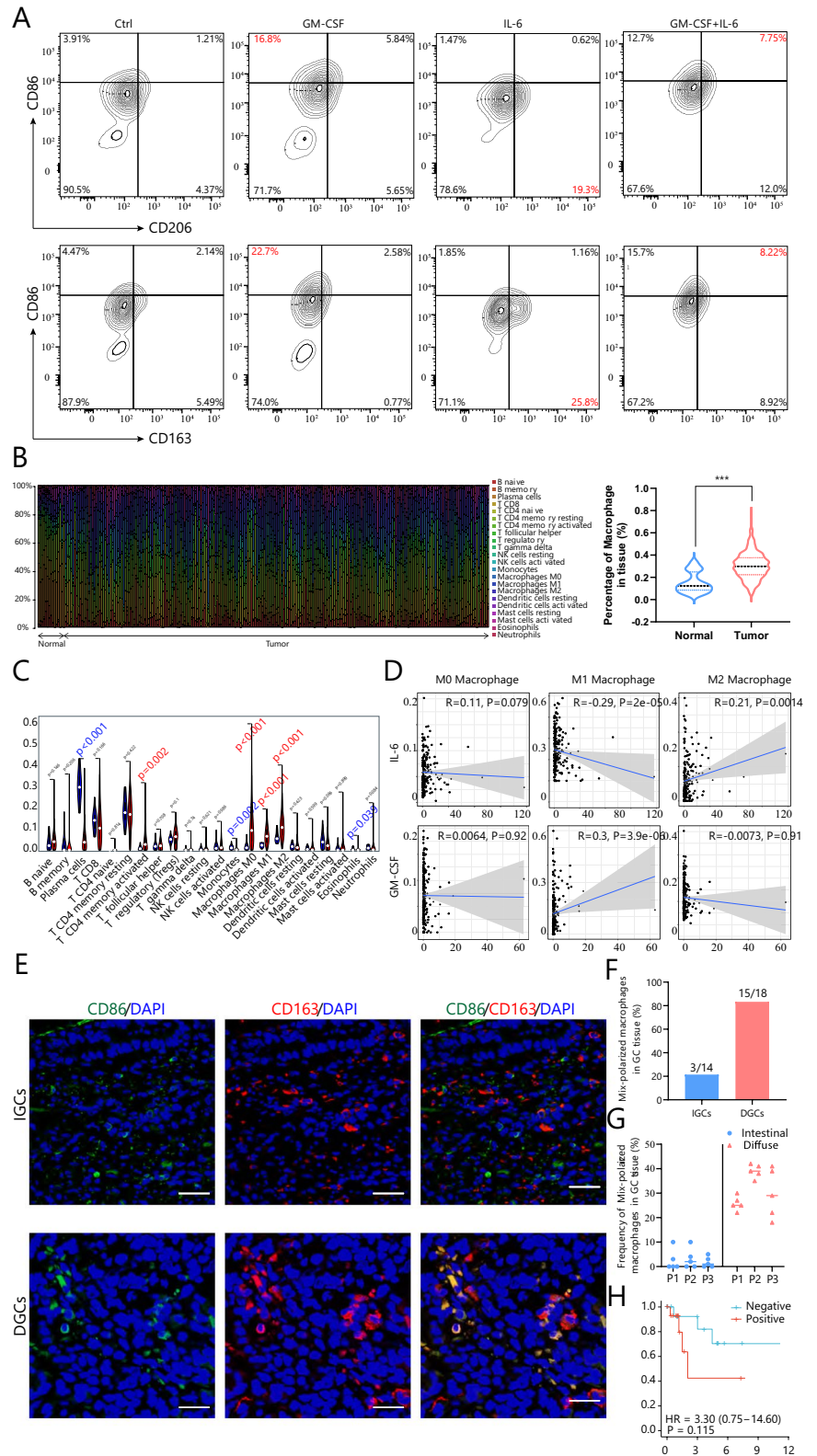
A previous study reported that CAF-derived IL-6 and GM-CSF promoted monocyte differentiation and induced TAM activation [24]. This finding was consistent with our results that IL-6 and GM-CSF were overexpressed in the "activated" NFs (Fig. 4A, B). Thus, we treated human macrophages with IL-6 and GM-CSF separately and simultaneously. CD86 was used to label M1-like macrophages, and CD163 and CD206 were used to label M2-like macrophages. Consistent with our expectations, under the sole action of GM-CSF, the proportion of M1-like macrophages was increased; IL-6 upregulated the proportion of M2-like macrophages. Under the combined effect of the two factors, the proportion of mixed-polarized macrophages was increased (Fig. 6A). This result revealed that the synergistic effect of NF-derived IL-6 and GM-CSF was critical for the induction of mixed-polarized macrophage polarization. To

further support our conclusion, we obtained transcriptome data from GC patients and normal controls from TCGA. CIBERSORT analysis suggested that immune infiltration recapitulated the immune clusters [25]. The proportion of macrophages was relatively low in normal samples but was increased significantly in GC samples (Fig. 6B).

Surprisingly, we found that in addition to the enrichment of M2-like macrophages, M1-like macrophages were also enriched in the GC samples (Fig. 6C). Although M1-like macrophages are traditionally recognized as a tumor-suppressive population, the population was significantly enriched in these GC samples. Macrophage polarization is often evaluated by a surface marker in cancer tissues. Thus, once molecules such as CD86 are recognized, these macrophages are classified as M1-like macrophages. We speculated that the "so-called" M1-like macrophages enriched in these cancerous tissues were not the pure M1-like type and that numerous mix-polarized macrophages were present, leading to this seemingly paradoxical phenomenon. Subsequent correlation analysis showed that IL-6 was positively correlated with M2-like macrophages and negatively correlated with M1-like macrophages; GM-CSF showed the opposite trend (Fig. 6D). This further supported the argument that these two molecules induce mixed polarization of macrophages.

To further confirm the existence and steady state of mixed-polarized macrophages in the TME, immunofluorescence staining was performed to detect macrophages in GC tissue. We assessed the existence of mixed-polarized macrophages in 32 GC patients, which included 14 IGC patients and 18 DGC patients. Surprisingly, we detected mixed-polarized macrophages in only 3 of 14 IGC samples (21.4%, Fig. 6E and F). However, this kind of macrophages was present in 15 of 18 DGC samples (83.3%, Fig. 6E and F). We randomly selected five fields/slide from the three mixed-polarized macrophage-positive IGC patients to evaluate the frequency of mixed-polarized macrophages (mixed-polarized macrophages vs. total macrophages). The rate did not exceed 10% in the IGC samples (Fig. 6G) but was approximately 30% in the DGC samples (Fig. 6G). Combined with the abovementioned influence of the TME on the malignant phenotype of DGCs. Subsequently, we analyzed the prognosis of these 32 GC patients. Although the sample size was limited, patients with mixed-polarized macrophages had a significantly worse prognosis than other patients (Fig. 6H). Comparing the general clinicopathological data of the two groups, not surprisingly, the presence of mixed-polarized macrophages was significantly associated with DGCs; sex was correlated with mixed-polarized macrophages, but this finding needs to be further explored due to sample size limitations. Other general clinicopathological data were not significantly different between the two groups (Supplement Table 2). These findings suggest

Fig. 6 NFs and DGC maintained the stability of mixed-polarized macrophages. **A.** Mixed-polarized macrophages were costained with CD86, CD163, and CD206 for 24 h after transfection with IL-6 and GM-CSF and then analyzed by flow cytometry. **B.** Normal- and tumor-infiltrating immune cell fractions estimated by CIBERSORT (left panel). The proportion of macrophages was increased in GC samples (right panel). **C.** Both M1 marker-positive and M2 marker-positive macrophages were enriched in GC tissues. **D.** IL-6 was positively correlated with M2 polarization and negatively correlated with M1 polarization; GM-CSF exhibited the opposite trend. **E.** IGC and DGC tissues were costained with CD86 and CD206 to identify mixed-polarized macrophages (green, CD86; red, CD163; blue, DAPI; scale bars, 25 μ m). **F, G.** Mixed-polarized macrophages were more enriched in DGCs than in IGCs. **H.** The existence of mixed-polarized macrophages was associated with the poor survival of GC patients



that mixed-polarized macrophages are a fundamental factor accounting for the protumoral behavior of GCs, especially DGCs.

Discussion

Increasing research advances have shed light on the cross-talk between the TME and malignant phenotypes [26]. Both malignant and nonmalignant cells in the TME can secrete various cytokines, microvesicles, and exosomes, thereby enhancing the interaction among cells, reshaping the micro-environment, and leading to cancer aggravation [27]. In fact, our previous studies demonstrated that the collapsed micro-environmental structure of DGCs contributed to the invasion of cancer cells [10]. The present study further identified the significance of reciprocal interactions between DGC cells and nonmalignant cells in the T0020ME.

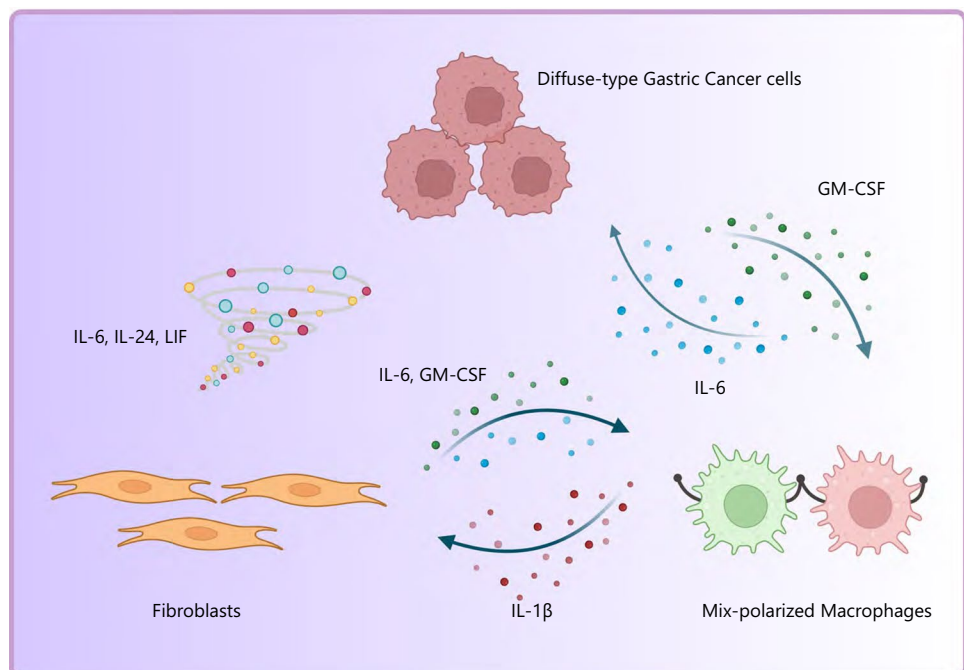
Macrophages, derived from PBMCs, were initially viewed as a vital link in innate immunity and a weapon for eradicating cancer cells. Macrophages can switch from one phenotype to another via a process called polarization, and these polarized cells differentially respond to microenvironmental stimuli and signals encountered in each specific tissue [28, 29]. Although macrophages are traditionally divided into M1-like and M2-like macrophages, their plasticity has been ignored, and they can indeed exist as a variety of phenotypes that differ from this classification [28]. To compensate for these dichotomous shortcomings, researchers further divided M2-like macrophages into four subtypes, M2a, M2b, M2c, and M2d, according to their profiles [30]. Although

the role of macrophages in normal and inflammatory tissues has gradually been refined, the subclassification of TAMs in the TME has not been detailed. To date, almost all studies have simply regarded TAMs as M2-like macrophages and identified them as CD163 and CD206. This understanding might be overly ambiguous, especially as TAMs are currently attractive therapeutic targets in clinical oncology [31]. Therefore, a deeper understanding of the subclassification of TAMs is needed.

Single-cell detection technology endowed us with the necessary technical support to analyze cell subpopulations in depth. Mass cytometry can be used to simultaneously measure multiple protein markers, divide cells into subgroups, construct a single-cell atlas of the tumor ecosystem, and link the cell landscape to its clinicopathological characteristics [32, 33]. Mass cytometry can also be used to reasonably distinguish tumor heterogeneity and provide a traceability method for identifying multicell interactions. Benefiting from this, we found that numerous macrophages in the triple co-culture system exhibited mixed polarization characteristics.

Under the action of the classic M1 inducer LPS and the classic M2 inducer IL-4, macrophages exhibit M1/M2 hybrid polarization. These mixed-polarizing macrophages can regulate ECM assembly and provide it with better plasticity [34]. Mix-polarized macrophages in lung cancer are associated with tissue-resident memory T-cell tumor infiltration and immunotherapy [35]. Moreover, the detection of alveolar macrophages in two human cohorts with different geographical locations and races (in the UK and Malawi) also revealed a large number of stable mix-polarized

Fig. 7 The reciprocal interaction between DGC cells and nonmalignant cells. Mixed-polarized macrophages facilitate the activation of NFs, which continue to promote the malignant phenotype of GC, and the TME maintains the steady state of mix-polarized macrophages.



macrophages [36]. In addition, the latest study on GC-associated single-cell RNA-seq (scRNA-seq) data reported a discrepancy between the transcriptional heterogeneity of macrophages and canonical M1/M2 classification [26]. Another scRNA-seq study reported the transition of nonmalignant cells in DGCs from a superficial to a deep distribution and changes in cytokine expression, revealing aggressive characteristics. However, the macrophage subclusters did not show distinct M1-like or M2-like features [37]. Multiple staining of GC tissues showed that macrophage density and marker expression varied between GC sample regions. The different marker expression profiles on macrophages were associated with their population disparity between the tumor site and non-tumor tissue and between the tumor-nest and stroma. From the cancer core to non-tumor, there was not a simple trend of conversion from M2-like to M1-like [38]. The subpopulation distribution and polarization status of macrophages observed between tumor nests and stromal compartments within different tumor regions could help to analyze their corresponding functions. Compared with the extreme M1 and M2 phenotypes, the mix-polarized macrophages might be the mainstay in the TME and represent a novel macrophage subtype involved in DGC progression.

Naturally, the potential molecular functions of mixed-polarized macrophages attracted our attention. Highly multiparametric analysis by mass cytometry revealed that the IL-1 β cytokine was expressed specifically in mixed-polarized macrophages. IL-1 β , a member of the interleukin 1 family, is mostly produced by activated macrophages as a proprotein, and caspase 1 participates in its activation [39]. Our previous studies showed that IL-1 β derived from activated macrophages suppresses 15-hydroxyprostaglandin dehydrogenase expression in pancreatic cancer cells [40] and three kinds of cytokines, including IL-1 β , endowed NFs with a CAF-like morphology by activating the NF- κ B pathway and promoted GC cell invasion [10, 41]. In this study, IL-1 β activated the NF- κ B pathway and promoted the transformation of NFs into CAF-like cells.

As we mainly focused on the communication between cells, we paid particular attention to the differential expression of cytokines and growth factors in IL-1 β -treated NFs in a comprehensive gene expression analysis. The IL-1 β -stimulated NFs exhibited increased secretion levels of IL-6, IL-24, LIF, and CSF2 (GM-CSF). Among these factors, the cancer-promoting effect of IL-6 is relatively straightforward [21], while the roles of IL-24 and LIF in GC remain controversial. For example, LIF has been shown to induce GC cell proliferation and invasion [42] but inhibit cancer stem cell tumorigenic properties via the Hippo-YAP pathway [43]. However, IL-6, IL-24, and LIF are all thought to be related to the activation of the JAK/STAT pathway [21–23], which is consistent with our results. In this study, we also confirmed the GC-promoting effect of the three proteins through

proliferation and migration assays. The biological function of LIF was relatively weak, which might explain the differential results among studies. The above results explained why the GC cells in the triple co-culture system were the most aggressive.

Evidence has shown that CAF-derived IL-6 and GM-CSF can induce monocyte to TAM polarization [24]. This study also showed that "activated" NFs promoted the expression of IL-6 and GM-CSF. Naturally, we used recombinant human IL-6 and GM-CSF to stimulate human-derived macrophages. Under the synergistic effect of the two cytokines, macrophages exhibited a mixed-polarized phenotype. TCGA transcriptome and immune cell subpopulation analyses revealed a correlation among GM-CSF, IL-6, and macrophage polarization. Exogenous IL-24 was shown to promote the secretion of GC-derived IL-18, which induced macrophage M1 polarization. This result indicates that the interaction between IL-6 and IL-24/IL-18 is also a potential factor that promotes mixed-polarized macrophage polarization [44]. The dynamic balance among different polarization-related factors is likely an essential factor that maintains the stability of the mix-polarized phenotype.

In summary, the TME is the core element that drives the development of GC. At the same time, TME components, including CAFs and TAMs, undergo subtle changes under the domestication of GC cells. Our study innovatively identified mixed-polarized macrophages in cancerous tissues, which may provide new ideas for further analyzing the mechanism of TAMs. Although IL-1 β , IL-6, and GM-CSF are well-known cytokines, the dynamic crosstalk among them has given them a new role in tumor progression. Mixed-polarized macrophages facilitate the activation of NFs, which continue to promote the malignant phenotype of GC, and the TME maintains the steady state of mix-polarized macrophages (Fig. 7). Therefore, the results herein provide novel insights into therapeutic strategies targeting the TME.

Supplementary Information The online version contains supplementary material available at <https://doi.org/10.1007/s10120-022-01352-3>.

Acknowledgements We thank S. Usuki (Liaison Laboratory Research Promotion Center, IMEG, Kumamoto University) for assisting with the RNA sequencing.

Author contributions J. Zhang: conceptualization, resources, data curation, software, formal analysis, validation, investigation, visualization, methodology, writing—original draft. L. Fu: investigation and methodology. A. Yonemura: resources, investigation, methodology. N. Yasuda: resources, investigation, methodology. F. Wei: resources. L. Bu: formal analysis and validation. X. Hu: resources. T. Akiyama: resources and methodology. F. Kitamura: investigation and methodology. T. Yasuda: investigation and methodology. T. Semba: writing—review and editing. T. Uchihara: investigation and methodology. R. Itoyama: investigation and methodology. K. Yamashita: formal analysis and validation.

K. Eto: resources. S. Iwagami: resources. M. Yashiro: resources. Y. Komohara: supervision, writing—review and editing. H. Baba: supervision, writing—review and editing. T. Ishimoto: conceptualization, data curation, formal analysis, supervision, funding acquisition, validation, investigation, visualization, methodology, writing—original draft, project administration, writing—review and editing.

Funding This work was supported by the Japan Society for the Promotion of Science (JSPS, KAKENHI grant nos. 20H03531, 20K09038, 20K08985, 20K08961, 21K16384 and 21K19535), the Naito Foundation, The Shinnihon Foundation of Advanced Medical Treatment Research, and the Inter-University Research Network for Trans-Omics Medicine program at the Institute of Molecular Embryology and Genetics at Kumamoto University.

Declarations

Conflict of interest The authors have no competing interests to disclose. Takatsugu Ishimoto is a member of the Editorial Board of the British Journal of Cancer.

Ethics approval and consent to participate Not applicable.

Consent to publish Not applicable.

References

1. Siegel RL, Miller KD, Jemal A. Cancer statistics, 2020. *CA Cancer J Clin.* 2020;70(1):7–30.
2. Ding N, Zou Z, Sha H, et al. iRGD synergizes with PD-1 knockout immunotherapy by enhancing lymphocyte infiltration in gastric cancer. *Nat Commun.* 2019;10(1):1336.
3. Kang YK, Boku N, Satoh T, et al. Nivolumab in patients with advanced gastric or gastro-oesophageal junction cancer refractory to, or intolerant of, at least two previous chemotherapy regimens (ONO-4538-12, ATTRACTION-2): a randomised, double-blind, placebo-controlled, phase 3 trial. *Lancet.* 2017;390(10111):2461–71.
4. Smyth EC, Nilsson M, Grabsch HI, et al. Gastric cancer. *Lancet.* 2020;396(10251):635–48.
5. Min J, Vega PN, Engevik AC, et al. Heterogeneity and dynamics of active Kras-induced dysplastic lineages from mouse corpus stomach. *Nat Commun.* 2019;10(1):5549.
6. Lauren P. The two histological main types of gastric carcinoma: diffuse and so-called intestinal-type carcinoma. An attempt at a histo-clinical classification. *Acta Pathol Microbiol Scand.* 1965;64:31–49.
7. The Cancer Genome Atlas Research Network. Comprehensive molecular characterization of gastric adenocarcinoma. *Nature.* 2014;513(7517):202–9.
8. Greten FR, Grivennikov SI. Inflammation and cancer: triggers, mechanisms, and consequences. *Immunity.* 2019;51(1):27–41.
9. Valkenburg KC, de Groot AE, Pienta KJ. Targeting the tumour stroma to improve cancer therapy. *Nat Rev Clin Oncol.* 2018;15(6):366–81.
10. Ishimoto T, Miyake K, Nandi T, et al. Activation of Transforming Growth Factor Beta 1 Signaling in Gastric Cancer-associated Fibroblasts Increases Their Motility, via Expression of Rhomboid 5 Homolog 2, and Ability to Induce Invasiveness of Gastric Cancer Cells. *Gastroenterology.* 2017;153(1):191–204. e16.
11. Gambardella V, Castillo J, Tarazona N, et al. The role of tumor-associated macrophages in gastric cancer development and their potential as a therapeutic target. *Cancer Treat Rev.* 2020;86:102015.
12. Murray PJ, Allen JE, Biswas SK, et al. Macrophage activation and polarization: nomenclature and experimental guidelines. *Immunity.* 2014;41(1):14–20.
13. Komohara Y, Fujiwara Y, Ohnishi K, et al. Tumor-associated macrophages: Potential therapeutic targets for anti-cancer therapy. *Adv Drug Deliv Rev.* 2016;99(Pt B):180–5.
14. Buechler MB, Fu W, Turley SJ. Fibroblast-macrophage reciprocal interactions in health, fibrosis, and cancer. *Immunity.* 2021;54(5):903–15.
15. Yashiro M, Chung YS, Nishimura S, et al. Peritoneal metastatic model for human scirrhous gastric carcinoma in nude mice. *Clin Exp Metastasis.* 1996;14(1):43–54.
16. Izumi D, Ishimoto T, Miyake K, et al. CXCL12/CXCR4 activation by cancer-associated fibroblasts promotes integrin β 1 clustering and invasiveness in gastric cancer. *Int J Cancer.* 2016;138(5):1207–19.
17. Yasuda T, Koiwa M, Yonemura A, et al. Protocol to establish cancer-associated fibroblasts from surgically resected tissues and generate senescent fibroblasts. *STAR Protoc.* 2021;2(2):100553.
18. Zeisel A, Hochgerner H, Lönnerberg P, et al. Molecular architecture of the mouse nervous system. *Cell.* 2018;174(4):999–1014.e22.
19. Sahai E, Astsaturov I, Cukierman E, et al. A framework for advancing our understanding of cancer-associated fibroblasts. *Nat Rev Cancer.* 2020;20(3):174–86.
20. Bu L, Baba H, Yoshida N, et al. Biological heterogeneity and versatility of cancer-associated fibroblasts in the tumor microenvironment. *Oncogene.* 2019;38(25):4887–901.
21. Johnson DE, O’Keefe RA, Grandis JR. Targeting the IL-6/JAK/STAT3 signalling axis in cancer. *Nat Rev Clin Oncol.* 2018;15(4):234–48.
22. Fickenscher H, Hör S, Küpers H, et al. The interleukin-10 family of cytokines. *Trends Immunol.* 2002;23(2):89–96.
23. Griffiths DS, Li J, Dawson MA, et al. LIF-independent JAK signalling to chromatin in embryonic stem cells uncovered from an adult stem cell disease. *Nat Cell Biol.* 2011;13(1):13–21.
24. Cho H, Seo Y, Loke KM, et al. Cancer-stimulated CAFs enhance monocyte differentiation and protumoral TAM activation via IL6 and GM-CSF secretion. *Clin Cancer Res.* 2018;24(21):5407–21.
25. Newman AM, Liu CL, Green MR, et al. Robust enumeration of cell subsets from tissue expression profiles. *Nat Methods.* 2015;12(5):453–7.
26. Sathe A, Grimes SM, Lau BT, et al. Single-cell genomic characterization reveals the cellular reprogramming of the gastric tumor microenvironment. *Clin Cancer Res.* 2020;26(11):2640–53.
27. Uchihara T, Miyake K, Yonemura A, et al. Extracellular vesicles from cancer-associated fibroblasts containing Annexin A6 induces FAK-YAP activation by stabilizing β 1 integrin, enhancing drug resistance. *Can Res.* 2020;80(16):3222–35.
28. Murray PJ. Macrophage Polarization. *Annu Rev Physiol.* 2017;79:541–66.
29. Okabe Y, Medzhitov R. Tissue-specific signals control reversible program of localization and functional polarization of macrophages. *Cell.* 2014;157(4):832–44.
30. Aiello I, Fedele MLM, Román F, et al. Circadian disruption promotes tumor-immune microenvironment remodeling favoring tumor cell proliferation. *Sci Adv.* 2020;6(42):eaaz4530.
31. Lin Y, Xu J, Lan H. Tumor-associated macrophages in tumor metastasis: biological roles and clinical therapeutic applications. *J Hematol Oncol.* 2019;12(1):76.

32. Anchang B, Davis KL, Fienberg HG, et al. DRUG-NEM: Optimizing drug combinations using single-cell perturbation response to account for intratumoral heterogeneity. *Proc Natl Acad Sci U S A*. 2018;115(18):E4294–303.
33. Cytlak U, Resteu A, Pagan S, et al. Differential IRF8 transcription factor requirement defines two pathways of dendritic cell development in humans. *Immunity*. 2020;53(2):353–70.e8.
34. Witherel CE, Sao K, Brisson BK, et al. Regulation of extracellular matrix assembly and structure by hybrid M1/M2 macrophages. *Biomaterials*. 2021;269:120667.
35. Garrido-Martin EM, Mellows TWP, Clarke J, et al. M1(hot) tumor-associated macrophages boost tissue-resident memory T cells infiltration and survival in human lung cancer. *J Immunother Cancer*. 2020;8(2):e000778.
36. Mitsi E, Kamng'ona R, Rylance J, et al. Human alveolar macrophages predominately express combined classical M1 and M2 surface markers in steady state. *Respir Res*. 2018;19(1):66.
37. Jeong HY, Ham IH, Lee SH, et al. Spatially distinct reprogramming of the tumor microenvironment based on tumor invasion in diffuse-type gastric cancers. *Clin Cancer Res*. 2021.
38. Huang YK, Wang M, Sun Y, et al. Macrophage spatial heterogeneity in gastric cancer defined by multiplex immunohistochemistry. *Nat Commun*. 2019;10(1):3928.
39. Petrasek J, Bala S, Csak T, et al. IL-1 receptor antagonist ameliorates inflammasome-dependent alcoholic steatohepatitis in mice. *J Clin Invest*. 2012;122(10):3476–89.
40. Arima K, Komohara Y, Bu L, et al. Downregulation of 15-hydroxyprostaglandin dehydrogenase by interleukin-1 β from activated macrophages leads to poor prognosis in pancreatic cancer. *Cancer Sci*. 2018;109(2):462–70.
41. Yasuda T, Koiwa M, Yonemura A, et al. Inflammation-driven senescence-associated secretory phenotype in cancer-associated fibroblasts enhances peritoneal dissemination. *Cell Rep*. 2021;34(8):108779.
42. Bian SB, Yang Y, Liang WQ, et al. Leukemia inhibitory factor promotes gastric cancer cell proliferation, migration, and invasion via the LIFR-Hippo-YAP pathway. *Ann N Y Acad Sci*. 2021;1484(1):74–89.
43. Seeneevassen L, Giraud J, Molina-Castro S, et al. Leukaemia Inhibitory Factor (LIF) inhibits cancer stem cells tumorigenic properties through hippo kinases activation in gastric cancer. *Cancers (Basel)*. 2020;12(8):2011.
44. Li J, Qin X, Shi J, et al. A systematic CRISPR screen reveals an IL-20/IL20RA-mediated immune crosstalk to prevent the ovarian cancer metastasis. *Elife*. 2021;10:e66222.

Publisher's Note Springer Nature remains neutral with regard to jurisdictional claims in published maps and institutional affiliations.

Springer Nature or its licensor (e.g. a society or other partner) holds exclusive rights to this article under a publishing agreement with the author(s) or other rightsholder(s); author self-archiving of the accepted manuscript version of this article is solely governed by the terms of such publishing agreement and applicable law.